

Asynchrony of Antarctic and Greenland climate change during the last glacial period

T. Blunier*, J. Chappellaz†, J. Schwander*, A. Dällenbach*, B. Stauffer*, T. F. Stocker*, D. Raynaud†, J. Jouzel‡, H. B. Clausen§, C. U. Hammer§ & S. J. Johnsen§||

* *Climate and Environmental Physics, Physics Institute, University of Bern, Sidlerstrasse 5, CH-3012 Bern, Switzerland*

† *CNRS Laboratoire de Glaciologie et Géophysique de l'Environnement (LGGE), BP 96, 38402 St Martin d'Hères Cedex, Grenoble, France*

‡ *Laboratoire des Sciences du Climat et de l'Environnement, UMR CEA-CNRS 1572, CEA Saclay, Orme des Merisiers, 91191 Gif sur Yvette, France*

§ *Department of Geophysics (NBI/APG), University of Copenhagen, Juliane Maries Vej 30, 2100 Copenhagen O, Denmark*

|| *Science Institute, Department of Geophysics, University of Iceland, Dunhaga 3, Is-107 Reykjavik, Iceland*

A central issue in climate dynamics is to understand how the Northern and Southern hemispheres are coupled during climate events. The strongest of the fast temperature changes observed in Greenland (so-called Dansgaard–Oeschger events) during the last glaciation have an analogue in the temperature record from Antarctica. A comparison of the global atmospheric concentration of methane as recorded in ice cores from Antarctica and Greenland permits a determination of the phase relationship (in leads or lags) of these temperature variations. Greenland warming events around 36 and 45 kyr before present lag their Antarctic counterpart by more than 1 kyr. On average, Antarctic climate change leads that of Greenland by 1–2.5 kyr over the period 47–23 kyr before present.

Greenland ice-core isotopic records^{1,2} have revealed 24 mild periods (interstadials) of 1–3 kyr duration during the last glaciation¹ known as Dansgaard–Oeschger (D–O) events³, where temperature increased by up to 15 °C compared with full glacial values^{4,5}. The temperature over Greenland is essentially controlled by heat released from the surface of the North Atlantic Ocean⁶. This heat is brought to the North Atlantic by the thermohaline circulation which is driven by the North Atlantic Deep Water (NADW) formation⁷. NADW strongly influences the deep circulation on a global scale. Therefore climate change related to the North Atlantic thermohaline circulation is not restricted to the North Atlantic region but has global implications⁸. Data correlating with D–O events have been found, for examples in the southern Atlantic⁹, the Pacific Ocean¹⁰ and probably also the Indian Ocean¹¹. On the continents, related events were found in North America where D–O events are manifested as wetter climate periods^{12,13}. Also, the hydrological cycle in the tropics appears to have changed in parallel with D–O events. This is indicated by changes in atmospheric methane concentration, the main source of which is wetlands situated in the tropics during the last glaciation¹⁴.

Temperature variations in Greenland inferred from the $\delta^{18}\text{O}$ record are characterized by fast warmings and slow coolings during the last glaciation. Antarctic temperature variations (from $\delta^{18}\text{O}$ and δD records) show a different pattern with fewer, less pronounced and rather gradual warming and cooling events over the same period^{15,16}.

One of the great challenges of climate research is therefore to find a mechanism that is able to reconcile the very different dynamical behaviour of high-latitude Northern and Southern hemispheres and their phase relationship during rapid climate change. A crucial test for our understanding of climate change is the relative phase of events in the two hemispheres. Using the global isotopic signal of atmospheric oxygen, Bender *et al.*¹⁷ hypothesized that interstadial events start in the north and spread to the south provided that they last long enough (~2 kyr), postulating that northern temperature variations lead those in Antarctica. On the other hand, they did not exclude the possibility that corresponding events are out of phase, as suggested by Stocker *et al.*¹⁸ on the basis of a simplified ocean–atmosphere model which shows that heat is drawn from the Antarctic region when NADW switches on at the onset of a D–O

event. This leads to a cooling of surface air temperatures in the south and a corresponding warming in the north. Charles *et al.*⁹ used stable-isotope ratios of benthic and planktonic foraminifera in a single core from the Southern Ocean to argue that the Northern Hemisphere climate fluctuations lagged those of the Southern Hemisphere by ~1.5 kyr. They conclude that a direct link of high-latitude climate is not promoted by deep-ocean variability.

Conclusive information regarding the phase lag of climate events can come only from high-resolution palaeoarchives which have either absolute or synchronized timescales with uncertainties smaller than 500 yr (for example, to distinguish the Younger Dryas from the Antarctic Cold Reversal¹⁹, hereafter YD and ACR). This prerequisite is at present satisfied only in polar ice cores. Here we use fast variations in methane during the last glaciation for a synchronization that permits a better estimate of the relative timing of events in the two hemispheres.

The CH_4 records from two Antarctic ice cores (Byrd station 80° S, 120° W; Vostok 78.47° S, 106.80° E) and one Greenland core (GRIP ice core, Summit 72.58° N, 37.64° W) have been used to establish coherent timescales for the Antarctic cores with respect to the GRIP timescale over the period from 50 kyr BP to the Holocene epoch. The timescale for the Greenland reference core (GRIP) has been obtained by stratigraphic layer counting²⁰ down to 14,450 yr BP with an uncertainty of ± 70 yr at 11,550 yr BP (termination of the YD). For older ages, the chronology is based on an ice-flow model²¹. This timescale is not considered to be absolute; for instance, the model-based dating differs from the stratigraphic layer counting in the deeper part of the core by several thousand years. However, our conclusions do not depend on the particular timescale, as explained below.

We are able to show that long-lasting Greenland warming events around 36 and 45 kyr BP (D–O events 8 and 12) lag their Antarctic counterpart by 2–3 kyr (comparing the starting points of corresponding warmings). On average, Antarctic climate change leads that of Greenland by 1–2.5 kyr over the period 47–23 kyr BP. This finding contradicts the hypothesis that Antarctic warmings are responses to events in the Northern Hemisphere¹⁷. The observed time lag also calls into question a coupling between northern and southern polar regions via the atmosphere, and favours a connection via the ocean. Indeed, climate models^{18,22–24} suggest that heat is extracted from the South-

ern Hemisphere when NADW formation switches on. This inter-hemispheric coupling is clearly identified in interstadial events 8 and 12, as well as during the termination of the last glaciation.

Synchronization of ice-core records

Because the porous firn layer on the surface of the ice sheet exchanges air with the overlying atmosphere, air, which gets enclosed in bubbles at 50–100 m below the surface (present-day conditions), has a mean age which is younger than the surrounding ice⁵. Consequently, a timescale for the ice and a timescale for the air need to be known, both of which depend on local climate characteristics. For GRIP, the difference between the age of the ice and the mean age of the gas at close-off depth (Δ age) has been calculated using a dynamic model⁵ for firn densification and diffusional mixing of the air in the firn, including the heat transport in the firn and temperature dependence of the close-off density. For Summit, estimates of the main parameters—accumulation rate and temperature^{4,25}—allow the calculation of Δ age with an uncertainty of only ± 100 yr between 10 and 20 kyr BP, increasing to ± 300 yr back to 50 kyr BP (ref. 5). Temperature was deduced from the $\delta^{18}\text{O}$ profile as suggested from borehole temperature measurements for the glacial–interglacial transition⁴, corresponding roughly to a linear dependence with a slope of 0.33‰ per °C. This relation is in contrast to today’s relation²⁶ with a slope of 0.67‰ per °C. However, there is good evidence that the $\delta^{18}\text{O}$ –temperature relation was close to the one derived from the borehole temperature profile throughout the past 40 kyr (ref. 5).

The model calculations are confirmed by an independent measurement of Δ age on the GISP2 core, drilled 30 km to the west of the GRIP drill site. A Δ age of 809 ± 20 yr was determined, on the basis of thermal fractionation of nitrogen at the termination of YD²⁷. This is consistent with Δ age of 775 ± 100 yr for the YD calculated with the same model used here⁵.

Two steps are necessary to synchronize ice cores via a gas record: (1) correlation of the CH₄ records, and (2) calculation of the age of the ice by determining Δ age. The initial GRIP CH₄ profile^{14,28} was refined between 9 and 55 kyr BP by an additional 180 samples measured both in the Bern and Grenoble laboratories, resulting in a mean sampling resolution of about 150 yr in the period of interest. A number of new samples were measured on the Antarctic cores from Byrd and Vostok station; 179 and 56, respectively. These

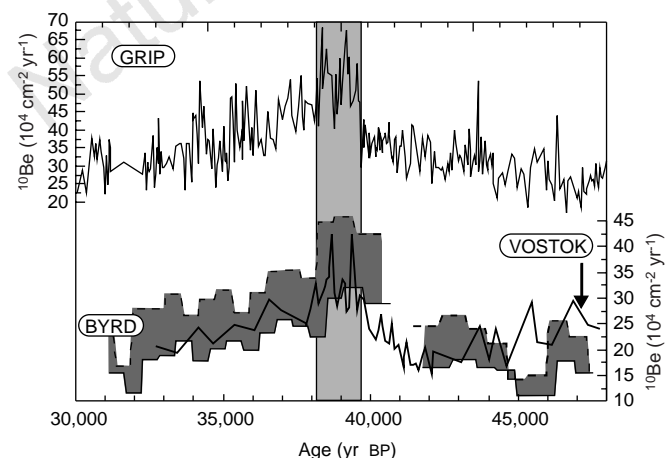


Figure 1 ¹⁰Be fluxes from Byrd³², Vostok³³ and GRIP³¹ ice cores. Values for Byrd were reduced by 15%, accounting for a difference in standards used for the measurements on the Byrd and the GRIP/Vostok cores (J. Beer, personal communication). Dating of the GRIP core is after ref. 21. For Byrd, two dating scenarios were used: lower temperature and accumulation (solid line); higher temperature and accumulation (dashed line; see Methods for details). Vostok was dated as described in Methods. The hatched area indicates the ¹⁰Be peak area deduced from the GRIP core.

measurements cover the time period 9–47 kyr BP on Byrd and 30–43 kyr BP on Vostok, with a mean sampling resolution of 200 and 250 yr, respectively. For the synchronization of the CH₄ records, a Monte Carlo method was used, searching for a maximal correlation between the records⁵. The fast CH₄ variations allow us to fit the records to ± 200 yr. The time period 25–17 kyr BP was excluded from the synchronization because only low CH₄ variations appear during that period, making the correlation uncertain.

The uncertainty in Δ age for the Antarctic sites is dominated by the uncertainty in temperature and accumulation. Estimates of the glacial–interglacial temperature difference at Vostok and Byrd station range from 7 to 15 °C (refs 29, 30). This range is covered in our Δ age calculations for Byrd station (see Methods). Δ age for the Byrd core is one order of magnitude smaller than for the Vostok core, and comparable to the GRIP Δ age. This makes the synchronization of isotopes more convincing for Byrd/GRIP than for Vostok/GRIP (see below and Methods).

To validate the resulting timescales, the distinct double peak of the cosmogenic radioisotope ¹⁰Be around 40 kyr BP can be used. The GRIP ¹⁰Be record³¹ is plotted together with that of Byrd³² on the new

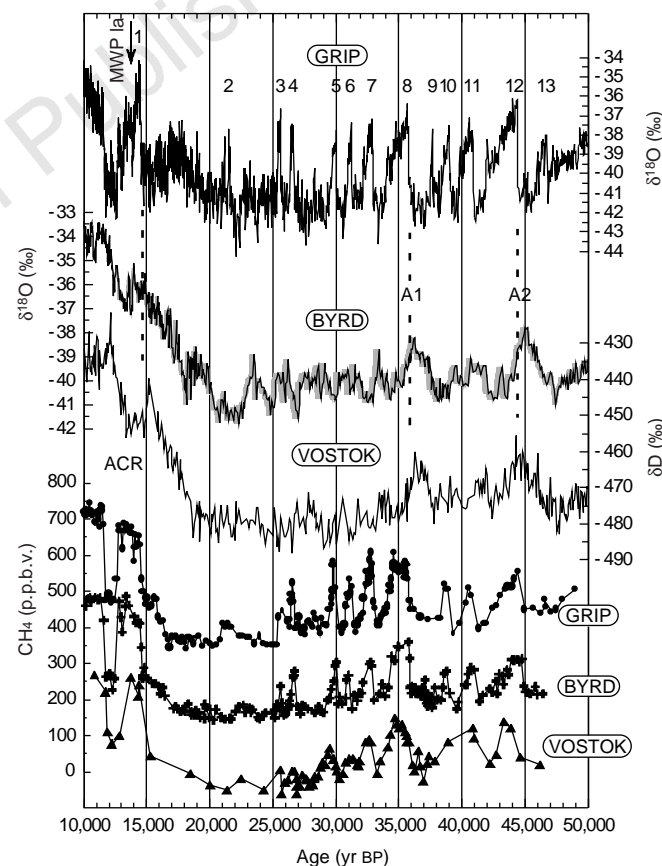


Figure 2 GRIP¹, Byrd¹⁵ and Vostok¹⁶ isotopic and CH₄ records on the common timescale (GRIP timescale in years before 1989). For the data from Byrd, a solid line shows the lower-temperature scenario, and the shaded area indicates the range of Δ age for the two temperature scenarios discussed in Methods. The CH₄ scale at lower left corresponds to the GRIP values; Byrd and Vostok values were lowered by 200 and 400 p.p.b.v., respectively, for better visibility. The numbers on top of the GRIP isotopic record indicate the location of Dansgaard-Oeschger events; ACR is the location of the Antarctic Cold Reversal as described by Jouzel *et al.*³⁴; Antarctic warmings are indicated by A1 and A2; vertical dashed lines show the location of Greenland warmings 1, 8 and 12 in the Antarctic cores. The Byrd $\delta^{18}\text{O}$ variation between 25 and 17 kyr BP shows most likely local climate characteristics because: (1) it is not seen in the Vostok or in the Dome C record²¹, and (2) it is not compatible with the climate mechanism seen during events A1, A2 and also the ACR present in all Antarctic records. The arrow marked MWP 1a indicates the position of the first meltwater pulse⁴⁵.

synchronized timescale in Fig. 1. Unfortunately, the resolution of the latter is much lower, which does not allow a firm validation. Nevertheless, the two timescales—resulting from assuming 7 °C or 15 °C glacial–interglacial temperature change—are both consistent with the ¹⁰Be signal. As they represent extreme positions relative to the GRIP record around the peak position, we are confident that the true Byrd timescale (relative to GRIP) lies within our estimates. The relative uncertainty at the location of the ¹⁰Be peak given by the two temperature models is about 300 yr.

Main features of Antarctic climate

Vostok station has a low accumulation rate and low temperature; the present values are 1.7–2.6 cm of ice per year and –55 °C, respectively¹⁶. This results in a large Δage, and makes Δage extremely sensitive to uncertainties in these parameters. Therefore, the Vostok CH₄ record alone is not well suited to correlate the Northern and the Southern hemispheres on a millennial scale. However, in combination with the detailed ¹⁰Be record^{31,33} a reasonable dating relative to Greenland can be achieved (for details, see Methods). The use of Vostok, in view of the relation between Greenland and Antarctic records, is to indicate which features seen in the Byrd core are representative for the climate in Antarctica (we limit our discussion to these features). They include the deglaciation and the ACR, a cold event occurring during the Bølling/Allerød^{19,34,35}, and warm events centring at 35.5 and 44.5 kyr BP (denoted as A1 and A2 in Fig. 2).

Phase lag

In Fig. 2 the isotopic records from Byrd (δ¹⁸O), Vostok (δD) and GRIP (δ¹⁸O), which is representative of Greenland^{2,21} and clearly registers Northern Hemispheric climate change³⁶, are plotted on the

common timescale (Table 1) based on GRIP. Our synchronization clearly demonstrates that the Antarctic warmings (A1 and A2) are out of phase with the corresponding D–O events (8 and 12). Antarctic temperature variations A1 and A2 are characterized by a gradual rather than abrupt increase and decrease; D–O events by a fast increase and a slow decrease. While the Antarctic temperature is already increasing, Greenland is still cooling. The Antarctic temperature rise is interrupted once Greenland temperature jumps to an interstadial state within only a few decades^{2,21}. Subsequently, the temperature decreases in both hemispheres to full glacial level, where Antarctica reaches this level earlier than Greenland.

We point out that our synchronization excludes the possibility that Antarctic and Greenland events are in phase. To bring the isotopic records in phase, the Byrd Δage would have to be reduced by more than 1,000 yr. As Δage is only about 500 yr during A1 and A2 (see Fig. 3) this would result in a negative Δage, which is impossible. Further, the relative position of A1 is also confirmed by the ¹⁰Be peak recorded in the ice of the three investigated cores.

Antarctic isotopic events other than A1 and A2 can hardly be allocated individually with D–O events. However, one can calculate the mean time shift required to obtain the best correlation between Greenland and Antarctic isotopic records in the period 45–23 kyr BP. Best correlations are obtained when the Antarctic signal is shifted towards younger ages by 1–2.5 kyr. This, and the timing of the events (A1 and A2), confirms the chronology obtained by deep sea cores⁹ and contradicts the hypothesis that long interstadials begin in the Northern Hemisphere and spread to Antarctica, creating a lag of Antarctic climate with respect to Greenland (at least for the past 50 kyr).

Implication for north–south connection

A connection between the hemispheres can take place over the ocean or over the atmosphere. Charles *et al.*⁹ suggested that both high northern and southern temperature could be driven over the atmosphere or the ocean by tropical temperature. Whereas coupling between Antarctic and tropical temperatures would be immediate, northern temperature would lag a tropical temperature change due to the thermal influence of the ice sheets or by the ice sheets' influence on salt balance of the North Atlantic surface layer. An immediate response of the Southern Hemisphere to tropical temperature would tend to synchronize the CH₄ (mainly related to tropical moisture changes) and the Antarctic isotope signal, whereas we observe a synchronism of CH₄ and Greenland δ¹⁸O (refs 5, 14). This makes a coupling via atmosphere improbable, and points instead to a dominant role of the ocean controlling the past climate of both polar regions.

Table 1 Corresponding depths for the three ice cores

Age of the ice (kyr BP)	Depth GRIP (m)	Depth Byrd† (m)	Depth Vostok‡ (m)
12	1638.0	1074.4	261.1
13	1674.0	1124.2	278.6
14	1722.6	1161.4	293.1
15	1770.0	1198.6	307.6
16	1802.2	1235.8	322.8
17	1834.3	1269.5	336.4
18	1867.6	1294.4	348.9
19	1894.5	1319.4	360.1
20	1916.5	1344.3	371.0
21	1937.7	1369.3	381.9
22	1958.8	1394.2	392.9
23	1975.6	1419.1	404.3
24	1993.1	1444.1	415.9
25	2011.1	1469.0	427.3
26	2031.6	1493.9	438.9
27	2051.6	1518.7	451.3
28	2065.1	1539.9	464.2
29	2079.9	1561.1	477.6
30	2097.5	1582.3	492.0
31	2112.6	1603.5	505.6
32	2129.5	1624.7	516.4
33	2149.9	1645.8	528.5
34	2162.9	1667.0	541.5
35	2182.7	1688.2	553.8
36	2203.6	1709.4	566.4
37	2214.7	1730.6	581.1
38	2227.5	1751.7	593.5
39	2242.8	1772.9	604.2
40	2255.1	1786.5	614.2
41	2272.0	1798.8	623.6
42	2282.6	1811.2	633.4
43	2297.6	1823.5	642.7
44	2315.9	1840.7	653.2
45	2330.2	1858.3	665.8
46	2340.2	1875.8	680.0
47	2353.2	1893.4	694.2

* The indicated depth corresponds to the higher Byrd temperature scenario (see Methods).
 † We note that in the new Byrd, as well as in the new Vostok, age–depth relations, rather unrealistic changes in the annual layer thickness appear. They result because the synchronization is based on the GRIP timescale which is, although well dated, not an absolute timescale. Therefore care must be taken when using the Byrd and Vostok timescales with respect to annual layer or accumulation changes. Our conclusions do not depend on an absolute timescale, and are unaffected by such problems (see Methods).

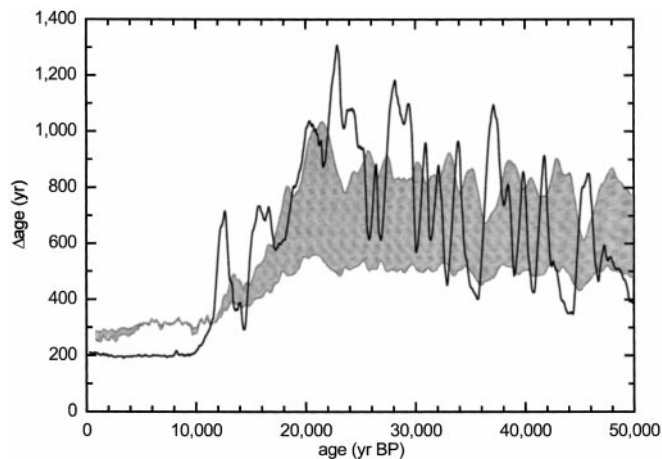


Figure 3 Plot of Δage versus ice age. The solid line shows data from GRIP⁵, the shaded area gives the range of Δage for the Byrd core covered by the temperature scenarios discussed in Methods, calculated with the same model as the GRIP Δage.

It is supposed that changes in the Atlantic thermohaline circulation, the direct cause of temperature changes in central Greenland⁶, are closely linked to ice-rafting events and associated melt water which occur simultaneously in the North Atlantic region³⁷. Melting reduces the deep-water formation and initiates cooling in the North Atlantic region. The cooling then slows the melting and permits re-establishment of the NADW formation, rapidly bringing heat to the North Atlantic⁶. The temperature increase then leads again to a freshwater input into the North Atlantic and to gradual shut down of NADW formation³⁸. Model simulations demonstrate the NADW's sensitivity to freshwater input in the North Atlantic^{24,39}, and they also indicate that the resumption of the 'conveyor belt' circulation after a shut-down is a rapid process^{39,40}.

D–O events and corresponding ice raftings occur more frequently than Antarctic warmings. Therefore, ice-rafting events can only partly, possibly through an increase in sea level, be initiated by Antarctic warmings. For the D–O events that have no counterpart in Antarctica, the trigger mechanism for ice-rafting events thus originates probably from an internal process of one of the ice sheets ablating into the North Atlantic. The Laurentide ice sheet can be excluded as it has a time constant of about 7 kyr (refs 41, 42), longer than the required 2–3 kyr between ice-rafting events³⁷. Bond and Lotti³⁷ proposed instead ice sheets in Greenland, the Barents Sea or Scandinavia as candidates for such a trigger mechanism.

Central to the dynamics that we reconstruct on the basis of the ice cores is the role of the thermohaline circulation in the North Atlantic. Activation of the thermohaline circulation in the North Atlantic tends to cool the Southern Hemisphere^{22,43}. This is exactly what happens during D–O events 12 and 8 (corresponding to A1 and A2), but also during D–O event 1, which is followed by the ACR¹⁹. Further, the YD/ACR out-of-phase relationship between Northern and Southern hemispheres is consistent with model simulations from ref. 18, recently reproduced with a three-dimensional coupled atmosphere–ocean general circulation model²⁴.

We may speculate that Antarctica is asynchronously coupled to the Northern Hemisphere during the whole glacial period investigated. Indeed, some of the smaller D–O events (for example, events 7 or 11) might have a concomitant cooling in Antarctica. The smaller amplitude of these coolings compared to the main events A1 and A2 might point to a positive correlation between the duration of a D–O event and the amplitude of the successive Antarctic cooling. However, it is also possible that the small Antarctic events may merely be noise in the isotopic records. In that case, the heat would only be drawn from Antarctica when Antarctica is in a warm phase. This leads to the speculation that under full glacial conditions Greenland and Antarctic temperature, and hence also thermohaline circulation and Antarctic circumpolar sea surface temperature⁹, are only weakly coupled. A weaker coupling of the hemispheres is achieved when the Atlantic thermohaline circulation exchanges less water with the Southern Ocean, and so has a reduced influence on the heat balance of the southern latitudes. The strength of this circulation also determines its stability to freshwater flux perturbations: a weaker thermohaline circulation is more likely to shut down for a given perturbation⁴⁴. If a weak Atlantic thermohaline circulation switches off, then the north will still experience strong cooling, but with a reduced influence on southern climate. We hypothesize that this is the case during the short D–O events which have no corresponding signal in Antarctic records. D–O events 12 and 8 and the Bølling/Allerød/YD sequence, on the other hand, would be examples of strong coupling between the hemispheres.

Warming in Antarctica tends to reduce sea surface density and hence the density of newly formed deep water. This favours NADW formation⁴³, and hence brings the ocean circulation closer to its strong mode with a tighter coupling of the circumpolar sea surface temperature to the Atlantic thermohaline circulation. A switch-on of the thermohaline circulation after ice-rafting events leads to the observed cooling in Antarctica, which results again in a weaker coupling of the

hemispheres for several thousand years. This is also consistent with an increased heat transport to high northern latitudes during A1 and A2 leading to the observed prolonged D–O events 8 and 12.

During the deglaciation, the climate system shows very similar behaviour. During the first part of the deglaciation the Antarctic warming is not interrupted as no ice-rafting events in the North Atlantic region are taking place: perhaps the lowered sea level makes it impossible for an ice sheet to initiate significant surging of other North Atlantic ice sheets. Then a sudden temperature increase in Greenland (14.5 kyr BP) initiates the same pattern as in the glaciation, namely a cooling in Antarctica (ACR). The first meltwater pulse (MWP 1A)⁴⁵ reduces NADW, at first gradually and then completely, allowing further warming in Antarctica. This makes the deglaciation a complicated process involving Milankovitch forcing, internal ice-sheet processes, and ocean circulation changes.

Further data from Antarctica which are synchronized with the existing records, together with model simulations, will help us disentangle the complicated pattern of climate change between Northern and Southern hemispheres for the entire glacial period. More, and better, data should be available from current European, Japanese and American ice-core drilling programmes. □

Methods

To calculate Δage, the accumulation rate and temperature need to be known. The temperature at the time of precipitation can be determined from the δ¹⁸O signal recorded in the ice. Assuming that today's spatial dependence between δ¹⁸O and temperature was also valid in the past, the glacial–interglacial temperature increase in Antarctica is ~7–10 °C (refs 16, 29). On the other hand, recent borehole temperature measurements at Vostok suggest³⁰ a temperature change of up to 15 °C.

The amount of snow falling over the year depends on the mean temperature of the inversion layer. This temperature (T₁) can be calculated for the surface temperature (T_G) according to⁴⁶:

$$T_1 = 0.67T_G - 1.2^\circ\text{C} \tag{1}$$

where T₁ and T_G are in °C. Assuming a linear relation between accumulation rate and the derivative of the water vapour partial pressure (P) with respect to temperature (T) (ref. 16), the accumulation rate which has led to a layer now found at depth z is given by:

$$a(z) = a_0 \left(\frac{\partial p}{\partial T} \Big|_{T_0} \right)^{-1} \frac{\partial p}{\partial T} \Big|_{T_1(z)} \tag{2}$$

where T₀ and T₁(z) are the inversion layer temperature for today's accumulation rate a₀ and for the past accumulation rate a(z), respectively.

Byrd. As the accumulation is calculated from the temperature and present accumulation rate, its uncertainty is essentially linked to the uncertainty in both parameters. For Byrd we have calculated a new age of the ice for two temperature scenarios. For the warmer scenario, the δ¹⁸O–temperature relation from ref. 29 was used (equation (3)); for the colder scenario³⁰ we use the linear relation given in equation (4):

$$T = (1.01^\circ\text{C per ‰})\delta^{18}\text{O} + 6.57^\circ\text{C} \tag{3}$$

$$T = (2.07^\circ\text{C per ‰})\delta^{18}\text{O} + 42.7^\circ\text{C} \tag{4}$$

From the two temperature scenarios, accumulation was calculated according to equations (1) and (2) with a₀ = 11.2 cm per yr ice equivalent⁴⁷. Thereafter, Δage was calculated using the dynamical model (Fig. 3) leading, in combination with the CH₄ synchronization, to a timescale for the warmer- and the colder-temperature scenario.

The accumulation rate is calculated from these temperatures and therefore also covers a wide range of possible accumulations (mean accumulation rates for the glacial are 7.9 and 5.5 cm yr⁻¹ for the higher- and the lower-temperature scenario, respectively). Alternatively, the accumulation rate can be calculated from the annual layer thickness, if the ice flow pattern is known. The flow pattern in the Byrd station area is very complicated (due to bedrock topography and melting at the bottom), which results in uncertainties in the calculated accumulation rate^{15,48}. However, our accumulation range over the glacial is consistent with measured annual layer thickness⁴⁷, assuming a linear thinning of annual layers with depth deduced from the Holocene period.

Vostok. As Vostok is a low accumulation site, the ice from the time period considered here is found in the upper 740 m of the ice sheet. There, ice flow is well known and was described by a glaciological model⁴⁹. Thus, it should in principle be possible to get coherency between the timescales for the ice and the occluded gas, accumulation and temperature. In a first approach the ¹⁰Be peak around 40 kyr was synchronized between GRIP³¹ and Vostok³³. For this purpose, accumulation rates were calculated from equations (1) and (2) from the isotopic temperature¹⁶. Δage was obtained using this accumulation and the isotopic temperature where the present-day accumulation rate *a*₀ was set to 2.1 cm yr⁻¹, within the uncertainty for today's accumulation rate⁵⁰. To obtain a timescale from the accumulation rate, annual layer thickness was calculated using the thinning function from the glaciological model⁴⁹. With this approach the main features in the isotopic record, as well as the Vostok CH₄ signal, appear shifted relative to the Byrd record. Reducing the Vostok temperature (suggested by Salamatin *et al.*⁵⁰) and therefore also accumulation rate would make the match even worse. In order to get the Vostok CH₄ record in agreement with its GRIP and Byrd counterpart, Vostok and/or the GRIP/Byrd timescales must be squeezed and stretched.

In a first case, we consider Vostok as reference timescale and adapt the GRIP/Byrd timescales. Consequently accumulation has to be changed in both cores and with the same amplitude and sign; therefore this does not change the relative phasing of GRIP and Byrd. This scenario brings event A2 in to agreement between Byrd and Vostok, but it creates fluctuations in the annual layer thickness of GRIP, which are not expected from the exponential relation between accumulation and δ¹⁸O (ref. 25).

In a second case, we consider GRIP as the reference timescale. The Vostok gas timescale is squeezed and stretched in order to fit the GRIP CH₄ record. The Vostok ice timescale is treated in the same way which is changing the accumulation rate. Thus Δage is re-calculated with the accumulation rates consistent with the modified timescale (using the thinning function from the glaciological model⁴⁹). The resulting change in the gas chronology was found to be negligible; this means that the Vostok CH₄ record is still in agreement with the GRIP CH₄ chronology. This scenario also brings event A2 into agreement between Byrd and Vostok, but now creates unexpected fluctuations in the annual layer thickness of Vostok. δ¹⁸O, ¹⁰Be and CH₄ data are presented using this chronology in Figs 1 and 2.

In both cases, maintaining consistency between ¹⁰Be peaks and CH₄ records, we obtain good correlation between the isotope records of Byrd and Vostok, and are therefore confident that the characteristic features reflect identical climate events. We are left with the unsolved problem of annual layer fluctuation either in the Vostok or in the GRIP ice core. However, the synchronization of the Byrd and GRIP core is robust to this problem.

Three cores from Vostok are involved in this study. The isotopic profile was obtained on the 3G core¹⁶ while ¹⁰Be was measured on the 4G core³³. The occurrence of a dust horizon in both cores at around 550 m depth (J. R. Petit, personal communication) allows an exact synchronization of the cores (4G depth increased by 3.41 m). The CH₄ profile was measured on the 5G core, which is of better quality than the 3G and 4G cores. The dust horizon at 550 m depth was not found in the 5G core. We thus performed additional CH₄ measurements on the 3G core over the CH₄ increase associated with D–O event 5, allowing us to estimate the depth offset between 3G and 5G (5G depth decreased by 3 m).

Received 1 September 1997; accepted 13 February 1998.

1. Dansgaard, W. *et al.* Evidence for general instability of past climate from a 250-kyr ice-core record. *Nature* **364**, 218–220 (1993).
2. Grootes, P. M., Stuiver, M., White, J. W. C., Johnsen, S. & Jouzel, J. Comparison of oxygen isotope records from the GISP2 and GRIP Greenland ice cores. *Nature* **366**, 552–554 (1993).
3. Oeschger, H. *et al.* in *Climate Processes and Climate Sensitivity* (eds Hansen, J. E. & Takahashi, T.) 299–306 (Vol. 29, Geophys. Monogr. Ser., Am. Geophys. Union, Washington DC, 1984).
4. Johnsen, S., Dahl-Jensen, D., Dansgaard, W. & Gundestrup, N. Greenland paleotemperatures derived from GRIP bore hole temperature and ice core isotope profiles. *Tellus B* **47**, 624–629 (1995).
5. Schwander, J. *et al.* Age scale of the air in the summit ice: Implication for glacial–interglacial temperature change. *J. Geophys. Res.* **102**, 19483–19494 (1997).
6. Bond, G. *et al.* Correlations between climate records from North Atlantic sediments and Greenland ice. *Nature* **365**, 143–147 (1993).
7. Roemmich, D. Estimation of meridional heat flux in the North Atlantic by inverse methods. *J. Phys. Oceanogr.* **10**, 1972–1983 (1981).
8. Broecker, W. S. & Denton, G. H. The role of ocean–atmosphere reorganizations in glacial cycles. *Geochim. Cosmochim. Acta* **53**, 2465–2501 (1989).
9. Charles, C. D., Lynch-Stieglitz, J., Ninnemann, U. S. & Fairbanks, R. G. Climate connections between the hemisphere revealed by deep sea sediment core/ice core correlations. *Earth Planet. Sci. Lett.* **142**, 19–27 (1996).
10. Behl, R. J. & Kennett, J. P. Brief interstadial events in the Santa Barbara basin, NE Pacific, during the

- past 60 kyr. *Nature* **379**, 243–379 (1996).
11. Bard, E., Rostek, F. & Sonzogni, C. Interhemispheric synchrony of the last deglaciation inferred from alkenone palaeothermometry. *Nature* **385**, 707–710 (1997).
12. Grimm, E. C., Jacobson, G. L. Jr, Watts, W. A., Hansen, B. C. S. & Maasch, K. A. A 50,000-year record of climate oscillations from Florida and its temporal correlation with the Heinrich events. *Science* **261**, 198–200 (1993).
13. Benson, L. V. *et al.* Climatic and hydrologic oscillations in the Owens Lake basin and adjacent Sierra Nevada, California. *Science* **274**, 746–749 (1996).
14. Chappellaz, J. *et al.* Synchronous changes in atmospheric CH₄ and Greenland climate between 40 and 8 kyr BP. *Nature* **366**, 443–445 (1993).
15. Johnsen, S. J., Dansgaard, W., Clausen, H. B. & Langway, C. C. Oxygen isotope profiles through the Antarctic and Greenland ice sheets. *Nature* **235**, 429–434 (1972).
16. Jouzel, J. *et al.* Vostok ice core: A continuous isotope temperature record over the last climatic cycle (160,000 years). *Nature* **329**, 403–408 (1987).
17. Bender, M. *et al.* Climate correlations between Greenland and Antarctica during the past 100,000 years. *Nature* **372**, 663–666 (1994).
18. Stocker, T. F., Wright, D. G. & Mysak, L. A. A zonally averaged, coupled ocean–atmosphere model for paleoclimate studies. *J. Clim.* **5**, 773–797 (1992).
19. Blunier, T. *et al.* Timing of the Antarctic Cold Reversal and the atmospheric CO₂ increase with respect to the Younger Dryas event. *Geophys. Res. Lett.* **24**, 2683–2686 (1997).
20. Hammer, C. U. *et al.* Report on the Stratigraphic Dating of the GRIP Ice Core (Spec. Rep. of the Geophysical Dept., Niels Bohr Institute for Astronomy, Physics and Geophysics, Univ. Copenhagen, in the press).
21. Johnsen, S. J. *et al.* Irregular glacial interstadials recorded in a new Greenland ice core. *Nature* **359**, 311–313 (1992).
22. Crowley, T. J. North Atlantic deep water cools the Southern Hemisphere. *Paleoceanography* **7**, 489–497 (1992).
23. Stocker, T. F. & Wright, D. G. Rapid changes in ocean circulation and atmospheric radiocarbon. *Paleoceanography* **11**, 773–796 (1996).
24. Schiller, A., Mikolajewicz, U. & Voss, R. The stability of the thermohaline circulation in a coupled ocean–atmosphere general circulation model. *Clim. Dyn.* **13**, 325–348 (1997).
25. Dahl-Jensen, D., Johnsen, S. J., Hammer, C. U., Clausen, H. B. & Jouzel, J. in *Ice in the Climate System* (ed. Peltier, W. R.) 517–532 (Springer, Berlin, 1993).
26. Johnsen, S. J., Dansgaard, W. & White, J. W. C. The origin of Arctic precipitation under present and glacial conditions. *Tellus B* **41**, 452–468 (1989).
27. Severinghaus, J. P., Sowers, T., Brook, E. J., Alley, R. B. & Bender, M. L. Timing of abrupt climate change at the end of the Younger Dryas interval from thermally fractionated gases in polar ice. *Nature* **391**, 141–146 (1998).
28. Blunier, T., Chappellaz, J., Schwander, J., Stauffer, B. & Raynaud, D. Variations in atmospheric methane concentration during the Holocene epoch. *Nature* **374**, 46–49 (1995).
29. Robin, G. de Q. in *The Climatic Record in Polar Ice Sheets* (ed. Robin, G. de Q.) 180–184 (Cambridge Univ. Press, London, 1983).
30. Salamatin, A. N. *et al.* Ice core age dating and paleothermometer calibration based on isotope and temperature profiles from deep boreholes at Vostok Station (East Antarctica). *J. Geophys. Res.* **103**, 8963–8978 (1998).
31. Yiou, F. *et al.* Beryllium 10 in the Greenland Ice Core Project ice core at Summit, Greenland. *J. Geophys. Res.* **102**, 26783–26794 (1997).
32. Beer, J. *et al.* *The Last Deglaciation: Absolute and Radiocarbon Chronologies* (eds Bard, E. & Broecker, W. S.) 141–153 (NATO ASI Ser. I 2, Springer, Berlin, 1992).
33. Raisbeck, G. M. *et al.* in *The Last Deglaciation: Absolute and Radiocarbon Chronologies* (eds Bard, E. & Broecker, W. S.) 127–140 (NATO ASI Ser. I 2, Springer, Berlin, 1992).
34. Jouzel, J. *et al.* The two-step shape and timing of the last deglaciation in Antarctica. *Clim. Dyn.* **11**, 151–161 (1995).
35. Sowers, T. & Bender, M. Climate records covering the last deglaciation. *Science* **269**, 210–214 (1995).
36. Siegenthaler, U., Eicher, U., Oeschger, H. & Dansgaard, W. Lake sediments as continental δ¹⁸O records from the transition of glacial–interglacial. *Ann. Glaciol.* **5**, 149–152 (1984).
37. Bond, G. C. & Lotti, R. Iceberg discharges into the North Atlantic on millennial time scales during the last deglaciation. *Science* **267**, 1005–1010 (1995).
38. Stocker, T. F. & Wright, D. G. The effect of a succession of ocean ventilation changes on radiocarbon. *Radiocarbon* **40**, 359–366 (1998).
39. Stocker, T. F. & Wright, D. G. Rapid transitions of the ocean's deep circulation induced by changes in surface water fluxes. *Nature* **351**, 729–732 (1991).
40. Wright, D. G. & Stocker, T. F. in *Ice in the Climate System* (ed. Peltier, W. R.) 395–416 (NATO ASI Ser. I 12, Springer, Berlin, 1993).
41. MacAyeal, D. R. A low-order model of the Heinrich event cycle. *Paleoceanography* **8**, 767–773 (1993).
42. MacAyeal, D. R. Binge/purge oscillations of the Laurentide ice sheet as a cause of the North Atlantic's Heinrich events. *Paleoceanography* **8**, 775–784 (1993).
43. Stocker, T. F., Wright, D. G. & Broecker, W. S. The influence of high-latitude surface forcing on the global thermohaline circulation. *Paleoceanography* **7**, 529–541 (1992).
44. Tziperman, E. Inherently unstable climate behaviour due to weak thermohaline ocean circulation. *Nature* **386**, 592–595 (1997).
45. Bard, E. *et al.* Deglacial sea-level record from Tahiti corals and the timing of global meltwater discharge. *Nature* **382**, 241–244 (1996).
46. Jouzel, J. & Merlivat, L. Deuterium and oxygen 18 in precipitation: modeling of the isotopic effects during snow formation. *J. Geophys. Res.* **89**, 11749–11757 (1984).
47. Hammer, C. U., Clausen, H. B. & Langway, C. C. Jr Electrical conductivity method (ECM) stratigraphic dating of the Byrd Station ice core, Antarctica. *Ann. Glaciol.* **20**, 115–120 (1994).
48. Whillans, I. M. Ice flow along the Byrd station strain network, Antarctica. *J. Glaciol.* **24**, 15–28 (1979).
49. Ritz, C. *Un Modèle Thermo-Mécanique d'évolution Pour le Bassin Glaciaire Antarctique Vostok-glacier Byrd: Sensibilité aux Valeurs des Paramètres Mal Connus*. Thesis, Univ. J. Fourier (1992).
50. Jouzel, J. *et al.* Extending the Vostok ice-core record of paleoclimate to the penultimate glacial period. *Nature* **364**, 407–412 (1993).
51. Lorius, C., Merlivat, L., Jouzel, J. & Pourchet, M. A 30,000-yr isotope climatic record from Antarctic ice. *Nature* **280**, 644–648 (1979).

Acknowledgements. This work, in the frame of the Greenland Ice Core Project (GRIP), was supported by the University of Bern, the Swiss National Science Foundation, the Federal Department of Energy (BFE), the Schwerpunktprogramm Umwelt (SPPU) of the Swiss National Science Foundation, the EC program "Environment and Climate 1994–1998", the Fondation de France and the Programm National de Dynamique du Climat of CNRS. We thank F. Finet for the CH₄ measurements on Vostok and part of GRIP, C. Rado and J. R. Petit for ice sampling at Vostok station, C. C. Langway for providing us with additional Byrd samples and F. Yiou, G. Raisbeck and J. Beer for the ¹⁰Be data.

Correspondence and requests for materials should be addressed to T.B. (e-mail: blunier@climate.unibe.ch).